Available online at www.sciencedirect.com

ScienceDirect

Mendeleev Commun., 2020, **30**, 241–243

Mendeleev Communications

Ignition of hydrogen–oxygen and stoichiometric hydrogen–methane–oxygen mixtures on hot wires at low pressures

Nikolai M. Rubtsov,*[a] Victor I. Chernysh,[a] Georgii I. Tsvetkov,[a] Kirill Ya. Troshin,[b] Igor O. Shamshin[b] and Alexander P. Kalinin[c]

[a] *A. G. Merzhanov Institute of Structural Macrokinetics and Materials Science, Russian Academy of Sciences, 142432 Chernogolovka, Moscow Region, Russian Federation. Fax: +7 495 962 8025; e-mail: nmrubtss@mail.ru*

[b] *N. N. Semenov Institute of Chemical Physics, Russian Academy of Sciences, 119991 Moscow, Russian Federation*

[c] *A. Yu. Ishlinsky Institute for Problems in Mechanics, Russian Academy of Sciences, 119526 Moscow, Russian Federation*

DOI: 10.1016/j.mencom.2020.03.038

It was found that the ignition temperatures of H_2–O_2 and H_2–CH_4–O_2 mixtures at a low pressure on heated Pd, Pt, Nichrome and Kanthal wires at 40 Torr increase with a decrease in H_2 concentration; only a heated Pd wire shows the pronounced catalytic action. Numerical calculations allowed us to reveal the role of an additional branching step, *viz.* $H + HO_2 \rightarrow 2OH$.

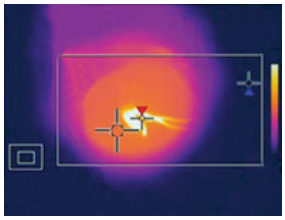

Keywords: ignition, temperature, hydrogen, methane, oxygen, heated wire, additional branching.

Hydrogen gas is promising as a non-polluting, renewable energy source of the future. However, certain problems concerning the safety of its production, transportation, and storage have to be resolved prior to its widespread use. One of the greatest fears is an accidental ignition, since hydrogen possesses much wider limits of flammability as compared to the most of conventional fuels.[1]

If one analyzes a risk of the accidental ignition in the case of an uncontrolled H_2 release (as may happen during a vehicle collision or a pipeline break), the most probable source of ignition will be a hot surface. It is important to be able to predict and thereby, to prevent conditions, under which the ignition can occur upon an exposure of the flammable mixture to a hot surface.

The fuel applications of H_2 require an ability to predictably ignite it. Supplying spark-ignition engines with hydrogen is problematic since the H_2–air mixture entering into the combustion chamber is susceptible to pre-ignition upon its contact with a hot surface such as intake valve. In the case of direct injection diesel engines, there is no any problem with the pre-ignition, but hydrogen is difficult to ignite by compression and thereby, some additional ignition source (*e.g.*, a glow plug) is required.[2] Therefore, the design of both spark-ignition and diesel engines should be based on the detailed knowledge about the ignition mechanism at a hot surface.

A number of experimental studies[3] have been performed in order to investigate the H_2 ignition at the hot surface. The most of measurements were recorded for gas mixtures under atmospheric pressure. Measurements of the surface temperature causing the H_2 ignition (T_{ign}) in air or O_2 at 1 atm have been usually ranged from 640 to 930 °C.[3,4] The Tign value as low as 70 °C was reported for H_2–air mixtures flowing over Pt wires, whereas catalytic effects were significant.[5,6] In addition, the dependence of T_{ign} on H_2 content was practically absent in certain published reportrs,[3,7] while in other works,[8] it was observed. We have previously demonstrated[9] that T_{ign} at 40 Torr over the heated Pd wire was lower by ~100 °C than that over a heated Pt wire. It was found for the thermal ignition that at pressures up to 180 Torr at 288 °C over Pd wire, the catalytic activity of surface was higher than that over Pt wire.[9] We have also found[10] that the dependence for H_2–CH_4–air mixes on reactor temperature was determined only by the H_2 fraction in the mixture, which additionally supports a presence of the dependence of T_{ign} on the H_2 concentration. The wide range of measured values evidences that the temperature of a hot surface required to launch ignition is not only a gas property, but also depends on various factors such as composition and pressure in the mixture, material and state of the surface (*viz.*, changes in temperature of the surface), *etc*.

In the present work, we investigated the ignition features for H_2–O_2 and H_2–CH_4–O_2 mixtures under low pressure at hot Pd, Pt, Nichrome and Kanthal wires† in order to verify an existence of the dependence of ignition temperature on the fuel concentration, and to estimate a contribution of the catalytic properties of used materials.

† Gases of chemically pure grade, Pt (purity of 99.99%), Pd (purity of 98.5%), and commercial Nichrome and Kanthal materials were used. The experiments were performed using H_2(100%), H_2(20%)–CH_4(80%), H_2(40%)–CH_4(60%), H_2(50%)–CH_4(50%), H_2(60%)–CH_4(40%) and H_2(80%)–CH_4(20%) stoichiometric gas mixtures with O_2 (*e.g.*, $2H_2 + O_2$). In some experiments, CH_4 was replaced with N_2. The reactor was a quartz cylinder 12 cm high and 8 cm in diameter, equipped with a removable CsI window at the butt-end of cylinder, inlets for gas blousing, pumping out and ignition of gas mixture (Figure S1 in Online Supplementary Materials). The reactor was used for observations of the initiated ignition, which was initiated by heating of polished Pd, Pt, Nichrome or Kanthal wires (0.3 mm in diameter and 80 mm long). The CsI optical window (40 mm in diameter and 5 mm thick) withstood only 5–6 impacts of ignitions at 40 Torr. A Flir 60 infrared camera (60 frames per second, 320×240 pix, sensitivity interval of

© 2020 Mendeleev Communications. Published by ELSEVIER B.V. on behalf of the N. D. Zelinsky Institute of Organic Chemistry of the Russian Academy of Sciences.

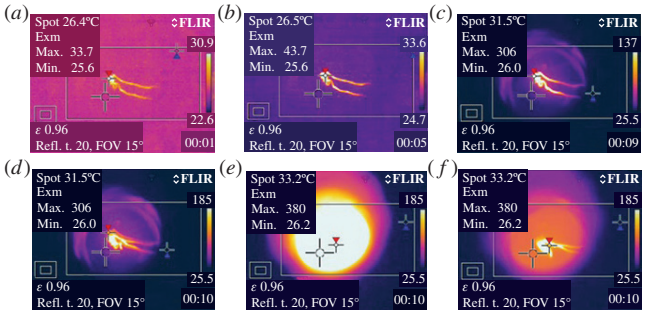

Figure 1 Detection of initiated ignition over heated Pd wire by the IR camera 60 frames per second, T_0 = 20 °C, H_2(60%)–CH_4(40%) mixed stoichiometrically with O_2, P_0 = 40 Torr. Time (in s) is given at the bottom right corner of each frame. Red triangle shows the maximum temperature in the rectangle, blue triangle shows minimum temperature in the rectangle, and the cross indicates the temperature at the point. The emissivity factor was set equal to 0.95 (to the lower left of the frame).

Temperatures of ignition at the heated wires were determined for the above mixtures. First of all, we have demonstrated that the replacement of CH_4 by N_2 does not cause any observable effect on the T_{ign} value, which is in a good agreement with our previous work.[10] Figure 1 shows images recorded in a typical experiment at the total pressure of 40 Torr. The temperature indicator of Flir 60 was somewhat delayed as compared to the rate of explosion; therefore, the maximum temperature [T_{exp} = 306 °C, see Figure 1(*c*),(*d*)] corresponds to that of the wire immediately before ignition. The temperature T_{exp} = 380 °C [see Figure 1(*e*)] corresponds to that of the wire heated with the flame. This temperature value is underestimated since the ignition proceeds fast, however the temperature during a delay period of the ignition can be measured precisely and consequently, it is reproducible. An emissivity factor in these experiments was set equal 0.95 (close to blackbody one). The recommended emissivity factor (ε) in the range of 8–14 mm is ~0.07 for Pd wire[11] and ~0.07–0.1 for Pt wire.[12] We have set an estimated values of ε ~ 0.1 for the both Pd and Pt wires, ε ~ 0.1 for Kanthal and ε ~ 0.15 for Nichrome wires.[13]

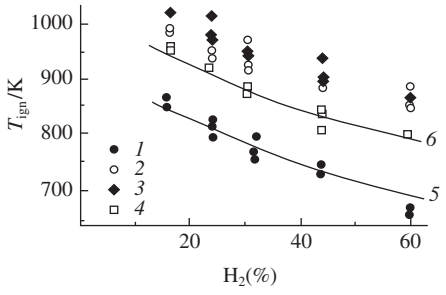

Figure 2 Experimental dependencies of T_{ign} over wires under investigation on H_2 content in the mixture, *1* – Pd, *2* – Pt, *3* – Nichrome, *4* – Kanthal. Curves present calculations with fitting values $k_{0cat} = 4\times10^{12}e^{-3500T^{-1}}$ cm^3 mol^{-1} s^{-1} for (*5*) Pd wire, and $k_{0cat} = 2\times10^{15}e^{-5000T^{-1}}$ cm^3 mol^{-1} s^{-1} for (*6*) Pt wire.

8–14 μm) was used to determine T_{ign} for the wires at the moment of ignition. To control the temperature values measured with Flir 60, an electric furnace as a blackbody radiation source (not shown in Figure S1) was placed near to the reactor. The readings of thermocouple placed into the furnace were almost the same as temperature values measured with Flir 60. A video recording was turned on at an arbitrary moment before initiation. A video file was saved in the computer memory, and its time-lapse processing was performed. The pumped reactor was filled with the gas mixture from a buffer volume up to necessary pressure. The wires were quickly heated to ignite the flammable mixture. Before each experiment, the reactor was evacuated down to 10^{-2} Torr. The total pressure in the reactor was monitored with a vacuum gauge; the pressure in the buffer volume was monitored with a manometer.

Evidently, a change in the emissivity from 0.1 to 0.15 changes the *T* values by dozens of *K*, so the uncertainties are taken into account hereinbelow. Figure 2 shows the actual ignition temperature for the mixtures at 40 Torr, estimated according to the Stefan–Boltzmann law ($0.95\ T^4\exp \approx \varepsilon \sim T^4_{ign}$). As one can see from these data, the dependence of T_{ign} on [H_2] exists, while Pd demonstrates the most pronounced catalytic activity (*i.e.*, the lowest T_{ign} values). These results are consistent with our previous work.[9]

The numerical investigations were performed in order to estimate the limiting ignition conditions (T_{ign}) at the wall temperature (300 K) for different H_2 contents in the mixtures. The proposed model reflects an experimental fact that at the initial steps of combustion process, a development of the initial center leads to the propagation of flame front[14] with the velocity *U*. A surface reaction of chain initiation as well as the specific features of the branched-chain mechanism for the H_2 oxidation were also taken into account. The reduced kinetic mechanism of H_2 oxidation under atmospheric and lower pressures can be represented by the following equations:[14]

$H_2 + O_2 \rightarrow 2\ OH$	$k_0 = 1.92\times10^{14}e^{-21890T^{-1}}$ cm^3 mol^{-1} s^{-1},	(0)
$OH + H_2 \rightarrow H_2O + H$	$k_1 = 4.63\times10^{12}e^{-2100T^{-1}}$ cm^3 mol^{-1} s^{-1},	(1)
$H + O_2 \rightarrow OH + O$	$k_2 = 1.99\times10^{14}e^{-8460T^{-1}}$ cm^3 mol^{-1} s^{-1},	(2)
$O + H_2 \rightarrow OH + H$	$k_3 = 1.88\times10^{14}e^{-6897T^{-1}}$ cm^3 mol^{-1} s^{-1},	(3)
$H + O_2 + M \rightarrow HO_2 + M$	$k_4 = 6.47\times10^{15}\ (T/298)^{-0.8}$ cm^6 mol^{-2} s^{-1},	(4)
$H + HO_2 \rightarrow 2\ OH$	$k_5 = 1.69\times10^{14}e^{-440T^{-1}}$ cm^3 mol^{-1} s^{-1},	(5)
$H_2 + HO_2 \rightarrow H_2O_2 + H$	$k_6 = 3\times10^{13}e^{-14400T^{-1}}$ cm^3 mol^{-1} s^{-1},	(6)
$OH + O \rightarrow H + O_2$	$k_7 = 9.29\times10^{12}$ cm^3 mol^{-1} s^{-1},	(7)
$O + HO_2 \rightarrow OH + O_2$	$k_8 = 3.25\times10^{13}$ cm^3 mol^{-1} s^{-1},	(8)
$OH + HO_2 \rightarrow H_2O + O_2$	$k_9 = 2.89\times10^{13}e^{-250T^{-1}}$ cm^3 mol^{-1} s^{-1},	(9)
$2\ HO_2 \rightarrow H_2O_2 + O_2$	$k_{10} = 2\times10^{12}$ cm^3 mol s,	(10)
$H_2O_2 + M \rightarrow 2\ OH + M$	$k_{11} = 1.3\times10^{17}e^{-22750T^{-1}}$ cm^6 mol^{-2} s^{-1},	(11)
$H + H + M \rightarrow H_2 + M$	$k_{12} = 2.2\times10^{15}$ cm^6 mol^{-2} s^{-1}.	(12)

Thus, the two-dimensional planar problem was examined. Characteristic scales of the process were chosen as follows: $t_0 = 1/(k_1^0[H_2]_0), x_0 = \{D_3/(k_1^0[H_2]_0)\}^{1/2}, U_0 = x_0/t_0 = \{D_3k_1^0[H_2]_0\}^{1/2}$ (the scales of time, length and velocity, respectively, whereas D_3 is the diffusivity of H_2). We have determined the following dimensionless variables and parameters: $\tau = t/t_0$, $\xi = x/x_0$, $\eta = y/y_0$, $\varpi = U/U_0$, Y_i = [concentration of the i^{th} component]/$[H_2]_0$, $\delta_i = D_i/D_3$ (D_i is diffusivity of the i^{th} component). Velocity and coordinates of the propagating flame front were expressed in terms of the diffusivity of H_2 (D_3): $\varpi = U/\{D_3\ k_1^0[H_2]_0\}^{1/2}$, $\xi = x/\{D_3/k_1^0[H_2]_0\}^{1/2}$, $\eta = y/\{D_3/k_1^0[H_2]_0\}^{1/2}$, wherein *U*, *x* and *y* are the corresponding dimensional values, k_1^0 is the preexponential factor for the reaction (1). Diffusivities (D_i/D_3, i = 0–6) δ_0, δ_1, δ_2, δ_3 =1, δ_4, δ_5, and δ_6 in an $H_2 + O_2$ mixture refer to OH, O, H, H_2, O_2, HO_2, H_2O_2 species, respectively. The set of reaction–diffusion equations for the above reaction mechanism takes the following form (*m* and *n* = 0–6 refer to OH, O, H, H_2, O_2, HO_2 and H_2O_2 reacting particles, respectively):

$$\partial Y_i/\partial\tau = \delta_i(\partial^2 Y_i/\partial\xi^2 + \partial^2 Y_i/\partial\eta^2) + \sum_{m\neq i,n} k_n Y_m Y_n - \sum_{m=i,n} k_n Y_m Y_n, \quad (13)$$

$$\partial T/\partial\tau = \delta_7(\partial^2 T/\partial\xi^2 + \partial^2 T/\partial\eta^2) + 1/(C_p\rho)\sum_{m,n} Q_n k_n Y_m Y_n. \quad (14)$$

The rate of heat release in the reaction chain[14] is given by equation (14). Herein, C_p is the mass-weighted mean specific heat capacity at a constant pressure, $\delta_7 \approx \delta_3$ is the thermal diffusivity of mixture for the near stoichiometric mixtures and $\delta_7 \approx \delta_4$ for the leaner mixtures,[11] *T* is the absolute temperature (K), ρ is the

known[15] density of mixture (g cm^{-3}). Specific heats Q_i and diffusivities were adopted from our previous work,[14] and f is the mole fraction of an initial component.

A reaction–diffusion equation for the O atoms as an example is given below:

$$\partial Y_1/\partial\tau = \delta_1(\partial^2 Y_1/\partial\xi^2 + \partial^2 Y_1/\partial\eta^2) + k_2Y_2Y_4 - k_3Y_1Y_3 - k_7Y_0Y_1 - k_8Y_1Y_5.$$

The solutions of set of 14 equations fulfill the following boundary conditions for the flame propagation from the right to the left; *i.e.* the flame propagation occurs if the flammable mixture is above the ignition limit (L is the distance between the axis and wall of reactor, symmetry conditions are specified along the axis):

$$Y_i(\xi,\eta) \to 0\ (i \neq 3,4);\ T(\xi,\eta) \to 300\ \text{K};\ \xi \to \pm\infty;$$
$$Y_3(\xi,\eta) \to f_{H_2};\ Y_4(\xi,\eta) \to f_{O_2};\ \xi \to -\infty;$$
$$\partial Y_3(\xi,\eta)/\partial\eta \to 0;\ \partial Y_4(\xi,\eta)/\partial\eta \to 0\ ;\ \xi \to +\infty;$$
$$[\partial Y_i(\xi,\eta)/\partial\eta]_L = 0;\ T(\xi,L) = 300\ \text{K}.$$

To solve the set, the initial fronts of starting components $Y_3[H_2]$ and $Y_4[O_2]$ at the time origin *vs.* coordinate were defined according to the composition of mixture. The two-step implicit scheme provided the second order of approximation for the system of equations over both spatial and time variables.[16] The shapes of fronts were approximated as $1/2 - 1/\pi[\text{arctg}(\xi + \eta)]$ (i = 3, 4), the initial front of T was specified as $T = T_{ign}e^{0.02(\xi + \eta)^2}$,[14] where T_{ign} is the examined value. These initial shapes correspond essentially to the initiation of flame propagation with an external source. The chosen shape of T had no effect on the steady state values of velocity of flame propagation.

Obviously, to initiate the ignition, a cycle of reactions including the branching (*i.e.*, an increase in the number of active centers) must occur.[17] To lower T_{ign}, *viz.* the ignition limit, the branching rate must increase,[17] *e.g.* at an expense of the additional branching step. Under the conditions of our experiments, this step is (5), wherein a relatively inactive HO_2 species turn into active OH ones, *i.e.* branching in addition to step (2) takes place. As has been previously demonstrated,[17] accounting for the reaction (5) allows one to explain an extension of the ignition area in the presence of external H atoms. In our case, the source of those atoms is a chain initiation step (0), since k_0 (*i.e.*, a and E) increases in the presence of a hot catalytic wire; it is designated below as k_{0cat} (a is a preexponent, E is activation energy). The more pronounced catalytic activity of wire is, the greater is the value of k_{0cat}. In the numerical experiment, the value of k_{0cat} ($k_{0cat} >> k_0$) for all the experimental points of each curve plotted in Figure 2 was processed according to the pairwise linear regression method[18] with parameters a and E, so the calculated curve was the closest to the experimental points. The experimental points on each curve were the mean of experimental temperature values, above which the combustion occurred and below which it did not exist. We draw attention to the qualitative nature of calculations due to many reasons, *e.g.* uncertainty in ε values and abbreviated character of the kinetic mechanism.

The profiles of chemical components were calculated: temperature and flame velocity U for one experimental point, which is between the combustion occurrence [Figure 3(*a*)] and combustion absence [Figure 3(*b*)]. According to Figure 3, the ignition occurs at initial T = 680 K, while there is no ignition at initial T = 670 K (the bloom of the color indicates spatial distributions of concentrations of Y_i, the color borders correspond to fixed concentrations, and a darker color corresponds to greater values of concentrations). The calculation results for the experimental points for Pd and Pt are shown in Figure 2 (curves).

As one can from Figure 2, accounting for the $H + HO_2 \to 2OH$ step provides an explanation of experimentally detected dependence of T_{ign} on H_2 concentration and allows one to obtain a good qualitative agreement with experimental data adjusting the values of k_{0cat} (a, E) for the catalytic heated wires: $k_{0cat} = 4\times10^{12}e^{-3500\pm1500\ T^{-1}}$ cm^3 mol^{-1} s^{-1} for epy Pd wire and $k_0 = 2\times10^{15}e^{-5000\pm1900\ T^{-1}}$ cm^3 mol^{-1} s^{-1} for Pt wire. It should be noted that only one of the possible factors responsible for lowering the initiation temperature in the presence of an effective catalyst has been qualitatively considered in the present work.

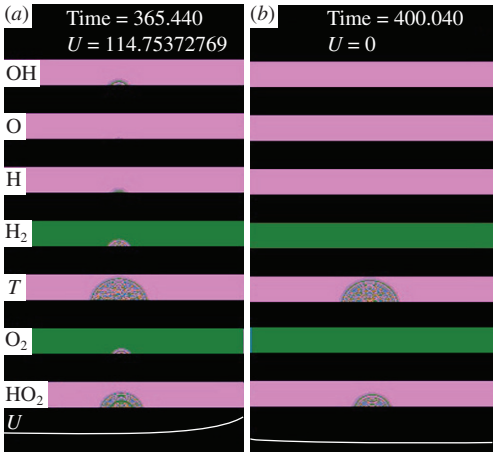

Figure 3 Calculated profiles for chemical components and temperature (*a*) above and (*b*) below T_{ign}. The top of each frame is the wall of reactor, and the bottom is the axis of the reactor. The flame front moves from the center to each side. P = 40 Torr, and wall temperature is 300 K. The flame velocity (U) is shown at the bottom in arbitrary units.

Online Supplementary Materials

Supplementary data associated with this article can be found in the online version at doi: 10.1016/j.mencom.2020.03.038.

References

1 M. Fisher, *Int. J. Hydrogen Energy*, 1986, **11**, 593.
2 A. B. Welch and J. S. Wallace, *SAE Tech. Pap. Ser. 902070*, 1990, doi:10.4271/902070.
3 R. K. Kumar, *Combust. Flame*, 1989, **75**, 197.
4 R. S. Silver, *Phil. Mag. J. Sci.*, 1937, **23**, 633.
5 K. B. Brady, *M. Sc. Thesis*, Cleveland, OH, 2010.
6 M. Rinnemo, O. Deutschmann, F. Behrendt and B. Kasemo, *Combust. Flame*, 1997, **111**, 312.
7 S. K. Menon, P. A. Boettcher, B.Ventura, G. Blanquart and J. E. Shepherd, *Western States Section of the Combustion Institute (WSSCI)*, 2012, Arizona University, Tempe, Paper # 12S-39.
8 D.-J. Kim, *Fire Sci. Eng.*, 2014, **28**, 8.
9 N. M. Rubtsov, V. I. Chernysh, G. I. Tsvetkov, K. Ya. Troshin, I. O. Shamshin and A. P. Kalinin, *Mendeleev Commun.*, 2018, **28**, 216.
10 N. M. Rubtsov, V. I. Chernysh, G. I. Tsvetkov, K. Ya. Troshin and I. O. Shamshin, *Mendeleev Commun.*, 2019, **29**, 469.
11 *Tables of Emissivity*, ZAO Euromix, Moscow, Russia, http://zaoeuromix.ru/tablicza-izluchatelnoj-sposobnosti.html (in Russian).
12 D. Bradley and A. G. Entwistle, *Brit. J. Appl. Phys.*, 1961, **12**, 670.
13 *Tables of Emissivity Factors for Materials*, OOO INCOL, Ekaterinburg, Russia, https://incoll.ru/primenenie/40-tablitsa-koeffitsientov-izlucheniya-materialov.htm (in Russian).
14 N. M. Rubtsov, *The Modes of Gaseous Combustion*, Springer International Publishing, Switzerland, 2016.
15 *Tablitsy fizicheskikh velichin* (*Tables of Physical Values*), ed. I. K. Kikoin, Atomizdat, Moscow, 1976 (in Russian).
16 G. I. Marchuk, *Metody vychislitel'noi matematiki* (*Methods of Computational Mathematics*), Nauka, Moscow, 1989 (in Russian).
17 N. N. Semenov, *O nekotorykh problemakh khimicheskoi kinetiki i reaktsionnoi sposobnosti* (*On Some Problems of Chemical Kinetics and Reactivity*), 2nd edn., AN SSSR, Moscow, 1958 (in Russian).
18 D. C. Montgomery, E. A. Peck and G. G. Vining, *Introduction to Linear Regression Analysis*, 5th edn., John Wiley and Sons, Hoboken, NJ, 2012.

Received: 11th July 2019; Com. 19/5981